Supporting Information for

A Mechanistic Study of the Oxidative Reaction of Hydrogen-Terminated Si(111) Surfaces with Liquid Methanol

Noah T. Plymale,[†] Mita Dasog,[†] Bruce S. Brunschwig,[‡] and Nathan S. Lewis*[,†,‡,§]

[†]*Division of Chemistry and Chemical Engineering,* [‡]*Beckman Institute*, and [§]*Kavli Nanoscience Institute*, *California Institute of Technology, Pasadena, California 91125, United States*

A. Supporting Figures.

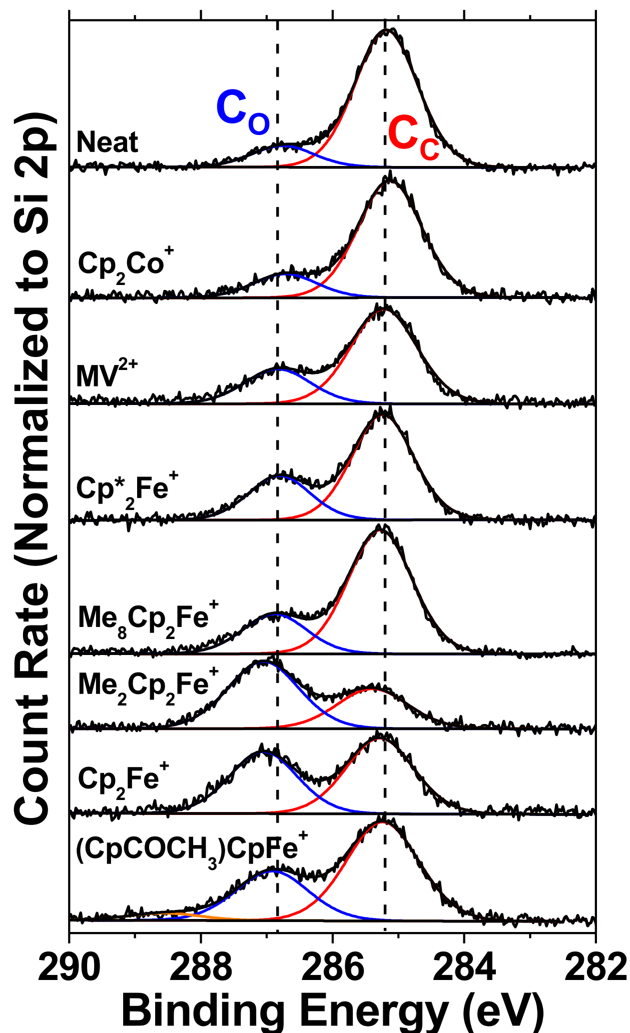

Figure S1. XPS data for the C 1s core level of H–Si(111) surfaces after 5 min exposure to neat CH_3OH or CH_3OH solutions containing 1.0 mM of the oxidant indicated above each spectrum. The approximate positions of the C bound to O (C_O) and C bound to C (C_C) peaks are indicated. The C_C peak arises from adventitious hydrocarbon species. The intensity of each spectrum was normalized to the Si 2p core level intensity, and the spectra are offset vertically for clarity.

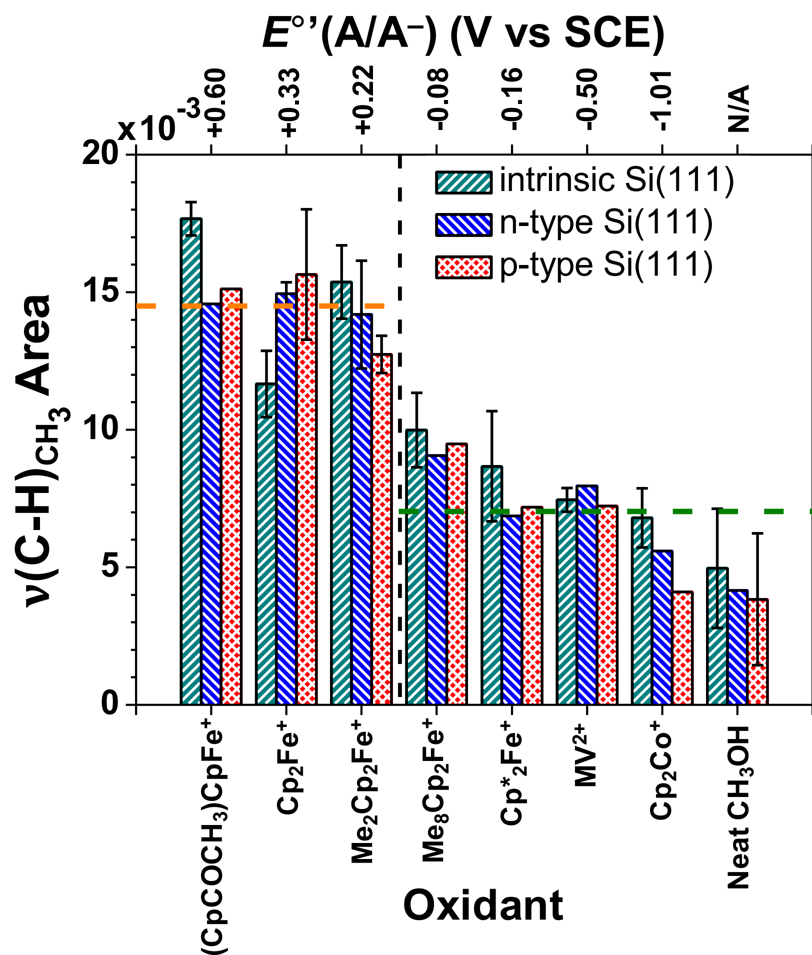

Figure S2. Correlation showing the area under the region containing the three $\nu(C\text{–}H)_{CH_3}$ peaks (3050–2800 cm^{-1}) as a function of the oxidizing conditions used in the reaction of H–Si(111) surfaces with CH_3OH in the absence of light. Reactions were performed for 5 min in neat CH_3OH or CH_3OH containing 1.0 mM of an oxidant. The experimentally determined formal potentials, $E°'(A/A^-)$, for each oxidant are given above the plot. The orange and green dotted lines are averages of the area under the $\nu(C\text{–}H)_{CH_3}$ peaks for all samples left and right of the black dotted line, respectively. Error bars represent statistical variation across multiple samples, and data points with no error bars represent single measurements. The error for single measurements can be estimated as $\pm 1 \times 10^{-3}$ based on the average standard deviation across all samples.

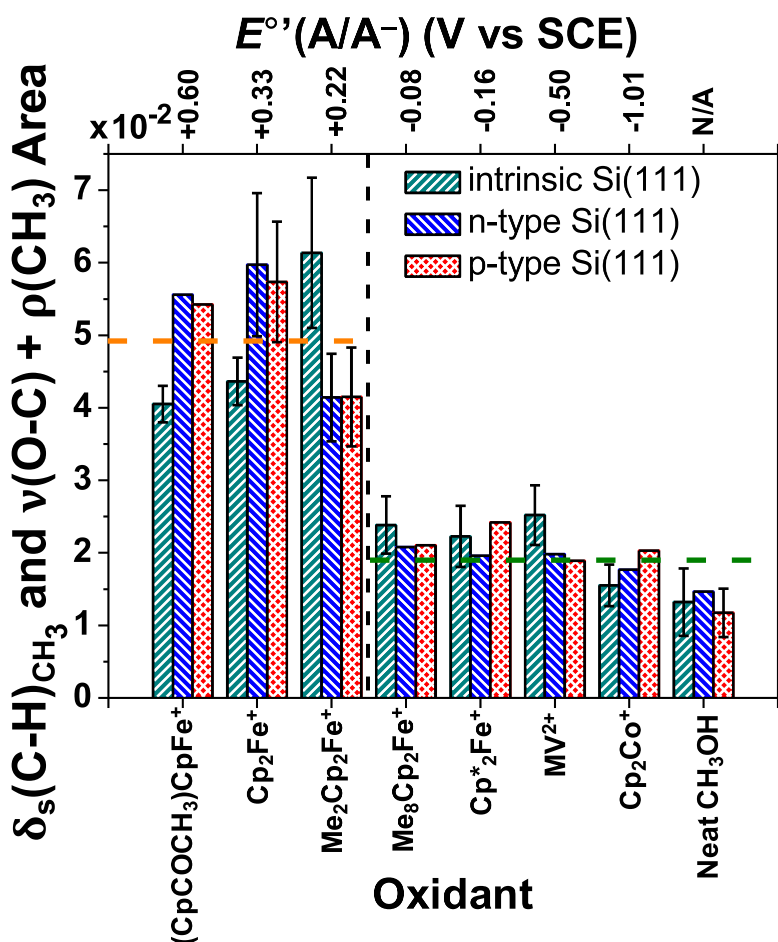

Figure S3. Correlation showing the area under the region containing the $\delta_s(C–H)_{CH_3}$ and ν(C–O) + $\rho(CH_3)$ peaks (1250–950 cm^{-1}) as a function of the oxidizing conditions used in the reaction of H–Si(111) surfaces with CH_3OH in the absence of light. Reactions were performed for 5 min in neat CH_3OH or CH_3OH containing 1.0 mM of an oxidant. The experimentally determined formal potentials, $E°'(A/A^-)$, for each oxidant are given above the plot. The orange and green dotted lines are averages of the area under the $\delta_s(C–H)_{CH_3}$ and ν(C–O) + $\rho(CH_3)$ peaks for all samples left and right of the black dotted line, respectively. Error bars represent statistical variation across multiple samples, and data points with no error bars represent single measurements. The error for single measurements can be estimated as $\pm 5 \times 10^{-3}$ based on the average standard deviation across all samples.

B. Analysis of F Content on H–Si(111) Surfaces Reacted in CH_3OH Solutions.

XPS detected the presence of F on a number of H–Si(111) samples after reaction with CH_3OH in the presence of an oxidant having a F-based counter ion (BF_4^-). Figure S4 presents representative high-resolution XPS data for the F 1s region of an intrinsic H–Si(111) sample exposed to CH_3OH containing $Me_2Cp_2Fe^+BF_4^-$. A photoemission signal at 686.2 eV was ascribed to free F^- and a photoemission signal at 687.4 eV was ascribed to BF_4^-.[1] The data indicate that a significant fraction of BF_4^- counter ion decomposed to yield F^- and BF_3, the latter being removed from the surface during rinsing. No residual Fe was detected from the oxidant on the surface, indicating that the observed F^- and BF_4^- was adsorbed to the surface upon reduction of the $Me_2Cp_2Fe^+$ species by the H–Si(111) surface to give neutral Me_2Cp_2Fe.

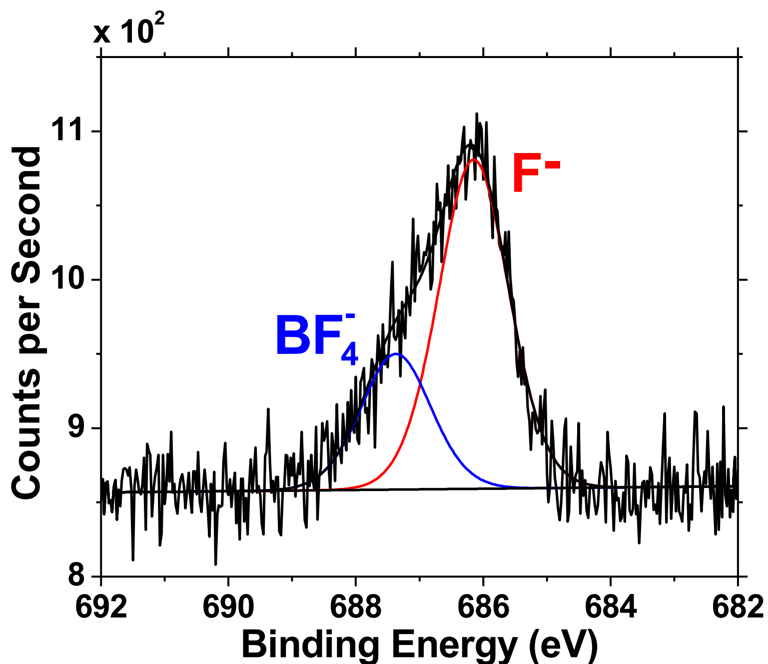

Figure S4. High-resolution XPS data for the F 1s region of an intrinsic H–Si(111) sample reacted with CH_3OH containing 1.0 mM $Me_2Cp_2Fe^+BF_4^-$ for 5 min in ambient light. The BF_4^- counter ion provided the source of the F detected.

The fractional monolayer coverage of F^- was calculated from high-resolution XPS data using eq S1:

$$\left(\frac{I_{\mathrm{F\ 1s}}}{I_{\mathrm{Si}}}\right)\left(\frac{SF_{\mathrm{Si}}}{SF_{\mathrm{F\ 1s}}}\right)\left(\frac{\rho_{\mathrm{Si}}}{\rho_{\mathrm{O}}}\right)=\left(\frac{1-e^{-\frac{d_{\mathrm{F}}}{\lambda_{\mathrm{F}}\sin\varphi}}}{e^{-\frac{d_{\mathrm{F}}}{\lambda_{\mathrm{Si}}\sin\varphi}}}\right) \quad \text{(S1).}$$

$I_{\mathrm{F\ 1s}}$ is the area under the F 1s photoemission peak (both peaks present in Figure S4), $SF_{\mathrm{F\ 1s}}$ is the sensitivity factor for the F 1s photoemission signal (1.00), ρ_{O} is the density of the terminating overlayer (assumed to be primarily hydrocarbon, giving ρ_{O} = 3.0 g cm^{-3}), and λ_{F} is the attenuation length of F 1s photoelectrons moving through a halogen overlayer (1.6 nm).[2] The remaining terms in eq S1 are defined for eq 3 in the main text. The thickness of the F layer d_{F} was determined using an iterative process, and the fractional monolayer coverage of F, θ_{F}, was calculated by dividing by the estimated thickness of 1 ML of F^- ions (0.13 nm).[3]

Figure S5 presents the analysis of the F 1s photoemission data from eq S1. F was observed primarily on samples that were reacted with CH_3OH containing Cp_2Fe^+ or $Me_2Cp_2Fe^+$. No detectable F signals were observed by XPS on surfaces reacted with CH_3OH containing $(CpCOCH_3)CpFe^+$, which was generated in situ prior to use, or $Cp_2Co^+PF_6^-$. Samples reacted with CH_3OH solutions containing $MV^{2+}2Cl^-$ did not exhibit detectable Cl by XPS. F was only observed in trace amounts on samples reacted with CH_3OH containing $Me_8Cp_2Fe^+$ or $Cp^*{}_2Fe^+$, and F was detected more often for these oxidants when the reactions were performed with illumination present. The data indicate that only samples reacted with CH_3OH under conditions that allow for oxidant-mediated methoxylation of the H–Si(111) surface exhibited detectable levels of F on the surface. This behavior provides evidence for the transfer of electrons to Cp_2Fe^+ or $Me_2Cp_2Fe^+$, leaving the BF_4^- and F^- (from decomposition of BF_4^-) counter ions associated with H^+ ions from the methoxylation reaction adsorbed to the surface.

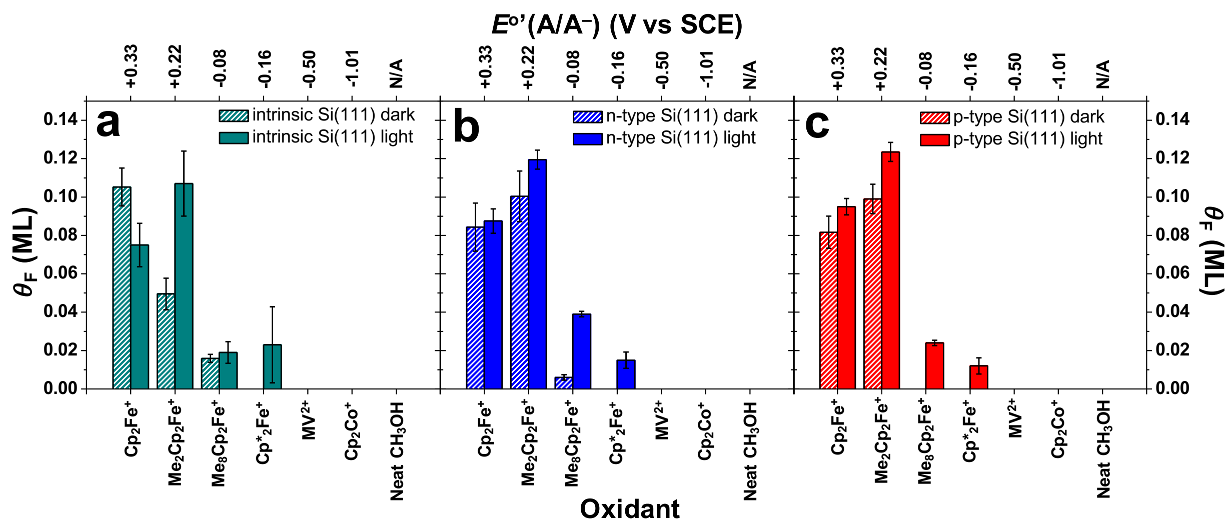

Figure S5. Correlation between θ_F and the oxidizing conditions used in the reaction of (a) intrisic, (b) n-type, and (c) p-type H–Si(111) surfaces with CH_3OH in the absence (striped) and presence (solid) of ambient light. Reactions were performed for 5 min in neat CH_3OH or CH_3OH containing 1.0 mM of an oxidant. Experimentally determined formal potentials, $E^{o\prime}(A/A^-)$, for each oxidant are given above each plot. The values for θ_F were determined by XPS measurements using eq S1.

C. Derivation of Equations 8–11.

The current density ratios presented in eqs 8 and 9 of the main text are derived below. The valence-band cathodic current density ($J_{\mathrm{vb,SR,C}}$) and anodic current density ($J_{\mathrm{vb,SR,A}}$) exchanging with the surface resonance are described by eqs S2 and S3, respectively.[4-5]

$$J_{\mathrm{vb,SR,C}} = -qN_{\mathrm{V}}k_{\mathrm{vb,SR,C}}\left[\mathrm{Si}^{+}\right] \quad \text{(S2)}$$

$$J_{\mathrm{vb,SR,A}} = qk_{\mathrm{vb,SR,A}}p_{\mathrm{s}}\left[\mathrm{Si}^{0}\right] \quad \text{(S3)}$$

Here, q is the unsigned elementary charge of an electron, N_{V} is the effective density of states in the valence band (cm^{-3}), p_{s} is the concentration (cm^{-3}) of holes in the valence band at the surface, $k_{\mathrm{vb,SR,C}}$ and $k_{\mathrm{vb,SR,A}}$ are the rate constants ($\mathrm{cm}^{3}\ \mathrm{s}^{-1}$) for cathodic and anodic charge transfer between the valence band and the surface resonance, respectively, and [Si^{+}] and [Si^{0}] are the concentrations (cm^{-2}) of the oxidized and reduced Si surface resonance states, respectively. Similarly, the conduction-band cathodic current density ($J_{\mathrm{cb,SR,C}}$) and anodic current density ($J_{\mathrm{cb,SR,A}}$) exchanging with the surface resonance are described by eqs S4 and S5, respectively.[4-5]

$$J_{\mathrm{cb,SR,C}} = -qk_{\mathrm{cb,SR,C}}n_{\mathrm{s}}\left[\mathrm{Si}^{+}\right] \quad \text{(S4)}$$

$$J_{\mathrm{cb,SR,A}} = qN_{\mathrm{C}}k_{\mathrm{cb,SR,A}}\left[\mathrm{Si}^{0}\right] \quad \text{(S5)}$$

Here, n_{s} is the concentration (cm^{-3}) of electrons in the conduction band at the surface, N_{C} is the effective density of states in the conduction band (cm^{-3}), and $k_{\mathrm{cb,SR,C}}$ and $k_{\mathrm{cb,SR,A}}$ are the rate constants ($\mathrm{cm}^{3}\ \mathrm{s}^{-1}$) for cathodic and anodic charge transfer between the conduction band and the surface resonance, respectively.

The Nernst equation relating the formal oxidation energy of the Si surface resonance ($\mathbf{E}^{\circ\prime}(\mathrm{Si}^{+/0})$) to the Nernstian oxidation energy of the surface ($\mathbf{E}(\mathrm{Si}^{+/0})$) can be written as

$$\frac{[\mathrm{Si}^{+}]}{[\mathrm{Si}^{0}]} = e^{\left(\frac{\mathbf{E}^{\circ\prime}(\mathrm{Si}^{+/0}) - \mathbf{E}(\mathrm{Si}^{+/0})}{k_{\mathrm{B}}T}\right)} \qquad \text{(S6)}$$

where k_{B} is Boltzmann's constant and T is the absolute temperature.

The ratio of the cathodic to anodic charge-transfer rate constants for the valence band and the conduction band are given in eqs S7 and S8, respectively.[6]

$$\frac{k_{\mathrm{vb,SR,C}}}{k_{\mathrm{vb,SR,A}}} = N_{\mathrm{V}} e^{\left(\frac{\mathbf{E}_{\mathrm{vb}} - \mathbf{E}^{\circ\prime}(\mathrm{Si}^{+/0})}{k_{\mathrm{B}}T}\right)} \qquad \text{(S7)}$$

$$\frac{k_{\mathrm{cb,SR,C}}}{k_{\mathrm{cb,SR,A}}} = \frac{1}{N_{\mathrm{C}}} e^{\left(\frac{\mathbf{E}_{\mathrm{cb}} - \mathbf{E}^{\circ\prime}(\mathrm{Si}^{+/0})}{k_{\mathrm{B}}T}\right)} \qquad \text{(S8)}$$

Here, $\mathbf{E}_{\mathrm{vb}}$ is the valence-band maximum energy and $\mathbf{E}_{\mathrm{cb}}$ is the conduction-band minimum energy.

Either at or away from equilibrium, the hole and electron concentrations at the semiconductor surface are related to the quasi-Fermi level positions according to eqs S9 and S10, respectively.[7]

$$p_{\mathrm{s}} = N_{\mathrm{V}} e^{\left(\frac{\mathbf{E}_{\mathrm{vb}} - \mathbf{E}_{\mathrm{F,p}}}{k_{\mathrm{B}}T}\right)} \qquad \text{(S9)}$$

$$n_{\mathrm{s}} = N_{\mathrm{C}} e^{\left(\frac{\mathbf{E}_{\mathrm{F,n}} - \mathbf{E}_{\mathrm{cb}}}{k_{\mathrm{B}}T}\right)} \qquad \text{(S10)}$$

The ratios of the cathodic current density to the anodic current density for the valence and conduction bands exchanging current with the surface resonance are defined as $|J_{\mathrm{vb,SR,C}}/J_{\mathrm{vb,SR,A}}| = R_{\mathrm{vb,SR}}$ and $|J_{\mathrm{cb,SR,C}}/J_{\mathrm{cb,SR,A}}| = R_{\mathrm{cb,SR}}$, respectively. $R_{\mathrm{vb,SR}}$ is expressed in terms of $\mathbf{E}_{\mathrm{F,p}}$ using eqs S2, S3, S6, S7, and S9 to yield

$$\left|\frac{J_{\mathrm{vb,SR,C}}}{J_{\mathrm{vb,SR,A}}}\right| = R_{\mathrm{vb,SR}} = e^{\left(\frac{\mathbf{E}_{\mathrm{F,p}} - \mathbf{E}(\mathrm{Si}^{+/0})}{k_{\mathrm{B}}T}\right)} \qquad \text{(S11)}$$

Similarly, $R_{\mathrm{cb,SR}}$ can be expressed in terms of $\mathbf{E}_{\mathrm{F,n}}$ using eqs S4, S5, S6, S8 and S10 to yield

$$\left|\frac{J_{\mathrm{cb,SR,C}}}{J_{\mathrm{cb,SR,A}}}\right| = R_{\mathrm{cb,SR}} = e^{\left(\frac{\mathbf{E}_{\mathrm{F,n}}-\mathbf{E}\left(\mathrm{Si}^{+/0}\right)}{k_{\mathrm{B}}T}\right)} \quad \text{(S12)}$$

As defined, conditions that lead to $R_{\mathrm{vb,SR}} > 1$ or $R_{\mathrm{cb,SR}} > 1$ indicate that the energetics at the interface favor reduction of the surface resonance, and $R_{\mathrm{vb,SR}} < 1$ or $R_{\mathrm{cb,SR}} < 1$ indicate that the energetics at the interface favor oxidation of the surface resonance. Eqs S11 and S12 are reproduced in the main text as eqs 8 and 9, respectively, to describe the flow of current at H–Si(111) surfaces undergoing oxidant-activated or potentiostatic methoxylation.

Following a similar derivation, the current density ratios presented in eqs 10 and 11 of the main text are derived below. The valence-band cathodic current density ($J_{\mathrm{vb,sol,C}}$) and anodic current density ($J_{\mathrm{vb,sol,A}}$) exchanging with the solution are described by eqs S13 and S14, respectively.[4-5]

$$J_{\mathrm{vb,sol,C}} = -qN_{\mathrm{V}}k_{\mathrm{vb,sol,C}}\left[\mathrm{A}\right] \quad \text{(S13)}$$

$$J_{\mathrm{vb,sol,A}} = qk_{\mathrm{vb,sol,A}}p_{\mathrm{s}}\left[\mathrm{A}^{-}\right] \quad \text{(S14)}$$

Here, [A] and [A^{-}] are the concentrations (cm^{-3}) of the molecular oxidant and reductant, respectively, in solution and $k_{\mathrm{vb,sol,C}}$ and $k_{\mathrm{vb,sol,A}}$ are the rate constants (cm^{4} s^{-1}) for cathodic and anodic charge transfer between the valence band and the solution, respectively. Similarly, the conduction-band cathodic current density ($J_{\mathrm{cb,sol,C}}$) and anodic current density ($J_{\mathrm{cb,sol,A}}$) are described by eqs S15 and S16, respectively.[4-5]

$$J_{\mathrm{cb,sol,C}} = -qk_{\mathrm{cb,sol,C}}n_{\mathrm{s}}\left[\mathrm{A}\right] \quad \text{(S15)}$$

$$J_{\mathrm{cb,sol,A}} = qN_{\mathrm{C}}k_{\mathrm{cb,sol,A}}\left[\mathrm{A}^{-}\right] \quad \text{(S16)}$$

Here, $k_{cb,sol,C}$ and $k_{cb,sol,A}$ are the rate constants (cm^4 s^{-1}) for cathodic and anodic charge transfer between the conduction band and the solution, respectively.

The Nernst equation can be rearranged to yield the relationship given in eq S17.

$$\frac{[\mathrm{A}]}{[\mathrm{A}^-]} = e^{\left(\frac{\mathbf{E}^{\circ\prime}(\mathrm{A/A^-}) - \mathbf{E}(\mathrm{A/A^-})}{k_\mathrm{B}T}\right)} \qquad \text{(S17)}$$

The formal solution energy is represented as $\mathbf{E}$°'(A/A$^-$)= $-qE$°'(A/A$^-$) and the Nernstian solution energy is represented as $\mathbf{E}$(A/A$^-$) = $-qE$(A/A$^-$). The ratio of the cathodic to anodic charge transfer rate constants for the valence band and the conduction band exchanging current with the solution are given in eqs S18 and S19, respectively.[6]

$$\frac{k_{\mathrm{vb,sol,C}}}{k_{\mathrm{vb,sol,A}}} = N_\mathrm{V} e^{\left(\frac{\mathbf{E}_\mathrm{vb} - \mathbf{E}^{\circ\prime}(\mathrm{A/A^-})}{k_\mathrm{B}T}\right)} \qquad \text{(S18)}$$

$$\frac{k_{\mathrm{cb,sol,C}}}{k_{\mathrm{cb,sol,A}}} = \frac{1}{N_\mathrm{C}} e^{\left(\frac{\mathbf{E}_\mathrm{cb} - \mathbf{E}^{\circ\prime}(\mathrm{A/A^-})}{k_\mathrm{B}T}\right)} \qquad \text{(S19)}$$

The ratios of the cathodic current density to the anodic current density for the valence and conduction bands exchanging current with the solution are defined as $|J_{vb,sol,C}/J_{vb,sol,A}| = R_{vb,sol}$ and and $|J_{cb,sol,C}/J_{cb,sol,A}| = R_{cb,sol}$, respectively. $R_{vb,sol}$ is expressed in terms of the $\mathbf{E}_{F,p}$ using eqs S9, S13, S14, S17, and S18 to yield

$$\left|\frac{J_{\mathrm{vb,sol,C}}}{J_{\mathrm{vb,sol,A}}}\right| = R_{\mathrm{vb,sol}} = e^{\left(\frac{\mathbf{E}_\mathrm{F,p} - \mathbf{E}(\mathrm{A/A^-})}{k_\mathrm{B}T}\right)} \qquad \text{(S20)}$$

Similarly, $R_{cb,sol}$ is expressed in terms of the $\mathbf{E}_{F,n}$ using eqs S10, S15, S16, S17, and S19 to yield

$$\left|\frac{J_{\mathrm{cb,sol,C}}}{J_{\mathrm{cb,sol,A}}}\right| = R_{\mathrm{cb,sol}} = e^{\left(\frac{\mathbf{E}_\mathrm{F,n} - \mathbf{E}(\mathrm{A/A^-})}{k_\mathrm{B}T}\right)} \qquad \text{(S21)}$$

As defined, conditions that lead to $R_{vb,sol} > 1$ or $R_{cb,sol} > 1$ indicates that the energetics at the interface favor reduction of species in solution, and $R_{vb,sol} < 1$ or $R_{cb,sol} < 1$ indicates that the energetics at the interface favor oxidation of species in solution. Eqs S20 and S21 are reproduced in the main text as eqs 10 and 11, respectively, to describe the flow of current at H–Si(111) surfaces undergoing oxidant-activated methoxylation.

Supporting Information References

1. Moulder, J. F.; Stickle, W. F.; Sobol, P. E.; Bomen, K. D., *Handbook of X-ray Photoelectron Spectroscopy: A Reference Book of Standard Spectra for Identification and Interpretation of XPS Data*; Physical Electronics USA, Inc.: Chanhassen, Minnesota, 1995.
2. Haber, J. A.; Lewis, N. S. Infrared and X-ray Photoelectron Spectroscopic Studies of the Reactions of Hydrogen-Terminated Crystalline Si(111) and Si(100) Surfaces with Br_2, I_2, and Ferrocenium in Alcohol Solvents. *J. Phys. Chem. B* **2002**, *106*, 3639-3656.
3. Plymale, N. T.; Ramachandran, A. A.; Lim, A.; Brunschwig, B. S.; Lewis, N. S. Control of the Band-Edge Positions of Crystalline Si(111) by Surface Functionalization with 3,4,5-Trifluorophenylacetylenyl Moieties. *J. Phys. Chem. C* **2016**, *120*, 14157-14169.
4. Kumar, A.; Santangelo, P. G.; Lewis, N. S. Electrolysis of Water at Strontium Titanate ($SrTiO_3$) Photoelectrodes: Distinguishing between the Statistical and Stochastic Formalisms for Electron-Transfer Processes in Fuel-Forming Photoelectrochemical Systems. *J. Phys. Chem.* **1992**, *96*, 834-842.
5. Lewis, N. S. An Analysis of Charge Transfer Rate Constants for Semiconductor/Liquid Interfaces. *Annu. Rev. Phys. Chem.* **1991**, *42*, 543-580.

6. Shreve, G. A.; Lewis, N. S. An Analytical Description of the Consequences of Abandoning the Principles of Detailed Balance and Microscopic Reversibility in Semiconductor Photoelectrochemistry. *J. Electrochem. Soc.* **1995**, *142*, 112-119.
7. Tan, M. X.; Laibinis, P. E.; Nguyen, S. T.; Kesselman, J. M.; Stanton, C. E.; Lewis, N. S., Principles and Applications of Semiconductor Photoelectrochemistry. In *Prog. Inorg. Chem.*, Karlin, K. D., Ed. John Wiley & Sons, Inc.: 1994; Vol. 41, pp 21-144.